

Optical glass-ceramics based on Fe^{2+} : MgAl_2O_4 nanocrystals and nucleated by TiO_2 and ZrO_2

Vasilisa S. Bukina^{1,a}, Olga S. Dymshits^{1,2,b}, Irina P. Alekseeva^{1,c},
Anna A. Volokitina^{1,d}, Svetlana S. Zapalova^{1,e}, Aleksandr A. Zhilin^{3,f}

¹Vavilov State Optical Institute, 36 Babushkina St., St. Petersburg, 192171, Russia

²Ioffe Institute, 26 Politekhnicheskaya, St Petersburg, 194021, Russia

³D.V. Efremov Institute of Electrophysical Apparatus, 3 Doroga na Metallostroi, pos. Metallostroi, St Petersburg, 196641, Russia

^anakara.oriyara@mail.ru, ^bvodym1959@gmail.com, ^cvgolub19@gmail.com,

^danna.itmo@gmail.com, ^ezenii99@yandex.ru, ^fzhilin1311@yandex.ru

Corresponding author: Olga S. Dymshits, vodym1959@gmail.com

PACS 78.67.Bf, 61.46.Hk, 42.70.Ce, 64.75.Jk, 81.10.Aj, 78.20.Ci

ABSTRACT Transparent glass-ceramics of magnesium aluminosilicate system based on Fe^{2+} : MgAl_2O_4 spinel nanocrystals nucleated by a mixture of TiO_2 and ZrO_2 and doped with 0.6 mol% FeO were developed. The glass was melted at 1580 °C with stirring and heat-treated in the temperature range from 800 to 1300 °C. The structure and spectroscopic properties of the glass and glass-ceramics were studied by DSC and XRD methods, Raman and absorption spectroscopy. ZrTiO_4 nanocrystals 6 nm in size precipitate during the nucleation heat-treatment at 800 °C. Spinel nanocrystals 9–14 nm in size are formed during heat-treatments at 850–1000 °C. Intense absorption at $\sim 2 \mu\text{m}$ is observed due to Fe^{2+} ions in tetrahedral positions in these crystals. Iron-doped sapphire crystallization in transparent glass-ceramics at 1000–1050 °C results in a decrease of absorption in this spectral range. The glass-ceramics are important for the development of saturable absorbers for the spectral range of 2–3 μm .

KEYWORDS Nanocrystals, spinel, transparent glass-ceramics, ferrous ions, nucleating agents.

ACKNOWLEDGEMENTS This work was partly supported by the Russian Science Foundation (Grant 23-23-00446).

FOR CITATION Bukina V.S., Dymshits O.S., Alekseeva I.P., Volokitina A.A., Zapalova S.S., Zhilin A.A. Optical glass-ceramics based on Fe^{2+} : MgAl_2O_4 nanocrystals and nucleated by TiO_2 and ZrO_2 . *Nanosystems: Phys. Chem. Math.*, 2023, **14** (6), 690–698.

1. Introduction

Nanosecond lasers emitting in the short-wave infrared spectral range of 2–3 μm can be used for range finding, remote sensing, medical applications, and meteorology. ZnS and ZnSe crystals doped with Fe^{2+} ions located in tetrahedral (T_d) sites are employed as saturable absorbers of such lasers [1]. Crystals of magnesium aluminate spinel with promising thermo-mechanical properties are alternative matrices for the accommodation of Fe^{2+} ions [2]. Glass-ceramics for optical applications are more cost efficient than corresponding single crystals and optical ceramics. They are easy and flexible in manufacturing and demonstrate high optical quality. Glass-ceramics, in contrast to glasses, have optical properties similar to those of the single crystals [3]. Magnesium aluminate spinel nanocrystals doped with Fe^{2+} ions were recently obtained in transparent glass-ceramics nucleated by titania, TiO_2 [4]. The drawback of glass-ceramics is that in these multiphase materials active ions are not only located in the desired crystal phase, but may also be distributed between and at the interfaces of different crystalline and amorphous phases. In [4] we demonstrated that in spinel-based magnesium aluminosilicate glass-ceramics, iron ions are distributed between the target spinel phase, the phase of the nucleating agent, magnesium aluminotitanate crystalline phase, and the residual highly siliceous glass. For the development of spinel-based glass-ceramics selectively doped with ferrous ions, Fe^{2+} , it is important to know how the nature of the nucleating agent influences the structure, phase composition and absorption properties of transparent spinel based glass-ceramics. The role of these agents was previously studied in the MgO – Al_2O_3 – SiO_2 ternary system [5], in which nucleation and internal bulk spinel crystallization is achieved using TiO_2 [6] or a mixture of TiO_2 and ZrO_2 [5, 7].

The aim of the present study is the development of transparent glass-ceramics of magnesium aluminosilicate system based on Fe^{2+} : MgAl_2O_4 spinel nanocrystals nucleated by a mixture of TiO_2 and ZrO_2 and the study of their structure and

spectral properties. In future, we are planning to compare the properties of these glass-ceramics with those nucleated by titania. These glass-ceramics are important for the development of saturable absorbers for the spectral range of 2–3 μm .

2. Experimental

2.1. Sample preparation

Model magnesium aluminosilicate glass with the composition (mol%) 20 MgO, 20 Al_2O_3 , 60 SiO_2 [6] was prepared with the addition of two nucleating agents, TiO_2 and ZrO_2 , [5, 7] and FeO. The nominal glass composition was (mol%) 18.1 MgO, 18.1 Al_2O_3 , 54.2 SiO_2 , 4.5 TiO_2 , 4.5 ZrO_2 , and 0.6 FeO.

The raw materials were reagent grade. The batch for producing 400 g of glass was melted in a crucible made of quartz ceramics at 1580 °C for 4 hours (h) with stirring. The glass was poured onto a cold metal plate and annealed at 660 °C. The transparent yellow glass, Fig. 1, was subjected to one- and two-stage secondary heat-treatments. The first nucleation stage was at 800 °C for 6 h and the temperature of the second stage ranged from 850 to 1300 °C with the same holding time of 6 h. As a result, transparent glass-ceramics were prepared by heat-treatments with the temperature of the second stage from 850 to 1050 °C. Their color changed with the heat-treatment temperature from the yellow to the brown, see Fig. 1. The glass heat-treated at the second stage at 1100 °C becomes translucent. The glass-ceramics prepared at 1200 and 1300 °C are opaque.

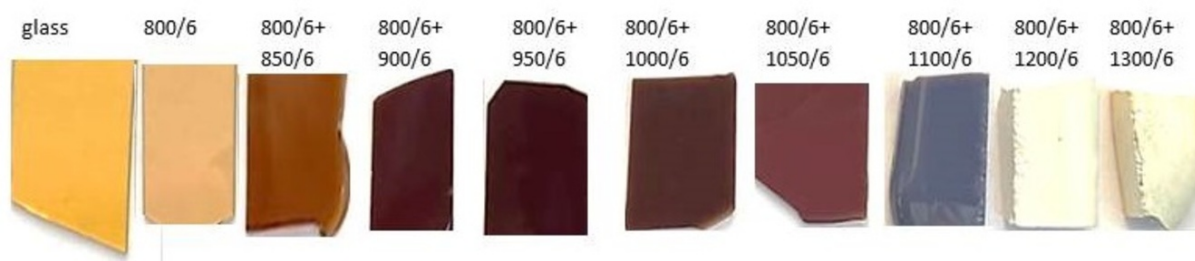


FIG. 1. Photographs of the polished glass, glass produced by the heat-treatment at 800 °C and glass-ceramics produced by two-stage heat-treatments with the first hold at 800 °C and the second hold from 850 to 1300 °C. Holding time at each stage is 6 h. The thickness of the polished samples is 1 mm.

2.2. Methods

XRD patterns of powdered samples were measured with a Shimadzu XRD-6000 diffractometer with nickel-filtered $Cu\ K\alpha$ radiation. The average crystal sizes were estimated from broadening of X-ray peaks according to Scherrer's equation [8]. The error in the average crystal size estimation is about 5%. The average size of $ZrTiO_4$ nanocrystals was estimated using the peak with Miller's indices (111); the size of magnesium aluminate spinel was estimated using the peak with indices (440). The average size of petalite-like phase was estimated using the peak with indices (211) and (210). The size of sapphirine of the 2M modification was estimated using the peaks with indices (122) and (1 10 0). The size of indialite crystals was estimated using the peak with Miller's indices (211), the size of cristobalite crystals was estimated using the peak with the indices (111). The unit cell parameter a was estimated from the position of the (440) plane of the spinel crystal.

Bulk samples of about 15 mg in weight were used for differential scanning calorimetry (DSC) study with help of a simultaneous thermal analyzer NETZSCH STA 449 F3 Jupiter with a dynamic flow atmosphere of Ar. The heating rate was 10 °C/min. The samples were the initial glass and the glass heat-treated at 800 °C for 6 h. For assigning the exothermic DSC peaks to certain crystalline phases, bulk samples of about 90 mg in weight were heated in the DSC furnace with the same heating rate of 10 °C/min up to the temperature of an appearance of a certain exothermic peak, cooled down to room temperature and subjected to powder XRD analysis.

Unpolarized Raman spectra were measured in backscattering geometry on an InVia (Renishaw, England) Micro-Raman spectrometer equipped with the multichannel detector cooled up to -70 °C. The spectra were excited by Ar+ CW laser line of 514 nm. Leica 50 \times (N.A. = 0.75) objective was used for illuminating the sample; the scattered light was collected by the same objective. Edge filter was placed before the spectrograph entrance slit; a spatial resolution was of 2 cm^{-1} . Every spectrum was averaged over 30 acquisitions with duration of 20 s.

Room-temperature absorption spectra were recorded by using a double-beam spectrophotometer Shimadzu UV 3600 in the range from 250 to 3300 nm. The samples were polished plates with a thickness of 1 mm. Absorbance spectra were normalized to the sample thickness.

3. Results and discussion

Figure 2 shows the DSC curve of the quenched glass and the curve of the same glass heat-treated at 800 °C for 6 h (the nucleation stage). From the DSC curve of the initial glass, the glass transition temperature, $T_g = 765$ °C, is determined. Several exothermic peaks associated with appearance of different crystalline phases are also observed. In the low temperature region, two exothermic peaks are formed, the crystallization onset temperatures, T_{on} , of which are $T_{on1} = 845$ °C and $T_{on2} = 918$ °C, and the crystallization maximum temperatures, T_{max} , are $T_{max1} = 877$ °C and $T_{max2} = 965$ °C. High-temperature exothermic peaks have complex shapes, the temperatures of their crystallization maxima are as follows: $T_{max3} = 1101$ °C, $T_{max4} = 1212$ °C, and $T_{max5} = 1290$ °C.

The glass transition temperature of the glass heat-treated at 800 °C for 6 h is higher than that of the initial glass, $T_g = 793$ °C. On the DSC curve of this sample, there is no peak in the range of 900 °C, observed on the DSC curve of the initial glass. In the region of high temperatures, the shapes and temperatures of maxima of exothermic peaks on the DSC curves of the initial and heat-treated glasses are near similar.

We determined the origin of the peaks for both DSC curves. After the crystallization maximum temperatures were found, the samples of the quenched glass and the glass preliminary heat-treated at 800 °C for 6 h, ~90 mg in weight, were heated in the DSC instrument up to the temperatures of the appearance of exothermic peaks. According to the XRD data, Fig. 3(a), the first exothermic peak in the DSC curve of the initial glass is associated with crystallization of zirconium titanate, $ZrTiO_4$, with orthorhombic structure. The sample heat-treated up to the temperature of the second exothermic peak (969 °C) has the phase composition of zirconium titanate and magnesium aluminate spinel, $MgAl_2O_4$, with the cubic structure, see Fig. 3(a).

An absence of the exothermic peak of $ZrTiO_4$ at ~880 °C on the DSC curve of the sample preheated at 800 °C for 6 h, see Fig. 2, suggests that almost all of $ZrTiO_4$ that crystallized during the heating of the initial glass in the DSC furnace, evolves during the preliminary heat-treatment of this glass at 800 °C for 6 h. This suggestion is confirmed by the similarity of the XRD patterns of the quenched glass heated in the DSC furnace up to 878 °C and the glass heat-treated in isothermal conditions at 800 °C for 6 h, see Fig. 4. The sample preheated at 800 °C for 6 h and heat-treated up to the temperature of the peak at 965 °C had the same phase composition as the quenched glass heated up to 969 °C. It is a mixture of zirconium titanate and magnesium aluminate spinel, see Fig. 3(b).

Taking into account the similarity of the high-temperature parts of the DSC curves of the both samples, we determined phase compositions only of the materials preheated at 800 °C for 6 h and heated in the DSC furnace to the temperatures of near 1300 °C, see Fig. 3(b). We believe the phase compositions of both materials heated up to these temperatures are similar.

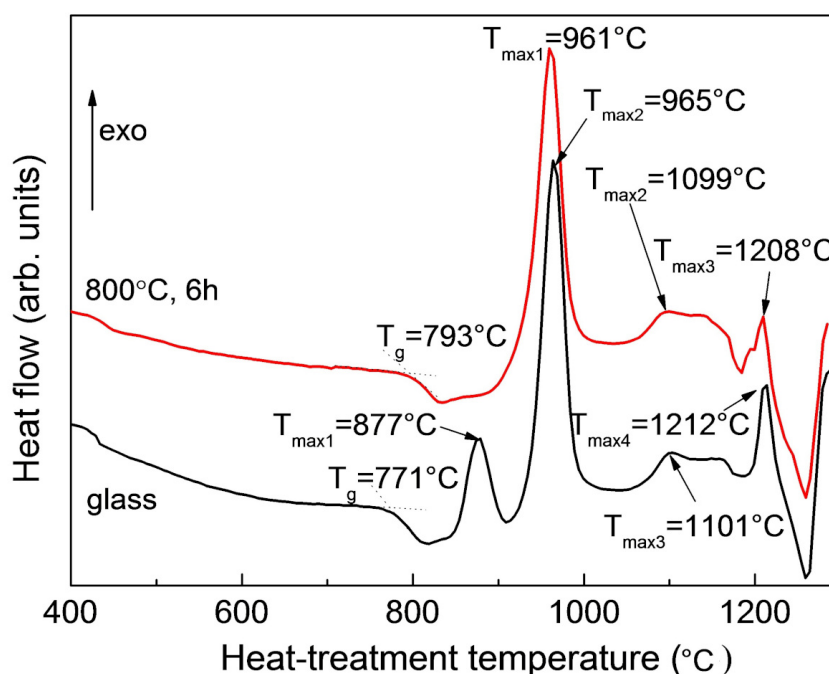


FIG. 2. DSC curves of the quenched glasses and the glass heat-treated at 800 °C for 6 h. T_g stands for the glass transition temperature, T_{max} stands for the maximum crystallization temperature. The curves are shifted for the convenience of observation

According to XRD data presented in Fig. 3(b), the broad exothermic peak in the temperature range from ~1100 to ~1200 °C is related to the transformation of magnesium aluminate spinel into sapphirine, the magnesium aluminosilicate

with monoclinic structure, which is in accordance with our previous study [4]. The preheated sample heat-treated up to the temperature of the T_{max4} (1212 °C) has a rich phase composition of the $ZrTiO_4$, sapphirine, and magnesium aluminosilicate with a quartz-like structure. The minimum on the DSC curve at about 1255 °C is related to the beginning of decomposition of the magnesium aluminosilicate with a quartz-like structure and appearance of traces of indialite, a high-temperature modification of cordierite. The sample also contained the crystals of $ZrTiO_4$ and sapphirine. The material heated to 1290 °C has the phase composition of $ZrTiO_4$, indialite, sapphirine, and traces of the magnesium aluminosilicate with a quartz-like structure.

The heat-treatments in isothermal conditions were conducted based on the results of the DSC–XRD study. According to the XRD patterns presented in Fig. 5, nanocrystals of zirconium titanate, $ZrTiO_4$, are formed during the heat-treatment at 800 °C for 6 h. Their average size is 6 nm, see Table 1. During heat-treatments at the second stage at temperature in the range from 850 to 1000 °C, magnesium aluminate spinel with average size of 8.5 – 13.5 nm is additionally formed. The variation of its unit cell parameter with heat-treatment is presented in Table 1. Traces of magnesium aluminosilicate with petalite structure with the average size of 16 nm are detected on the XRD pattern of the sample obtained by the heat-treatment at the second stage at 850 °C. In the temperature range from 1000 to 1100 °C, sapphirine crystals with the average size from 17 to 25 nm are formed at the expense of spinel, the intensity of zirconium titanate peaks increases.

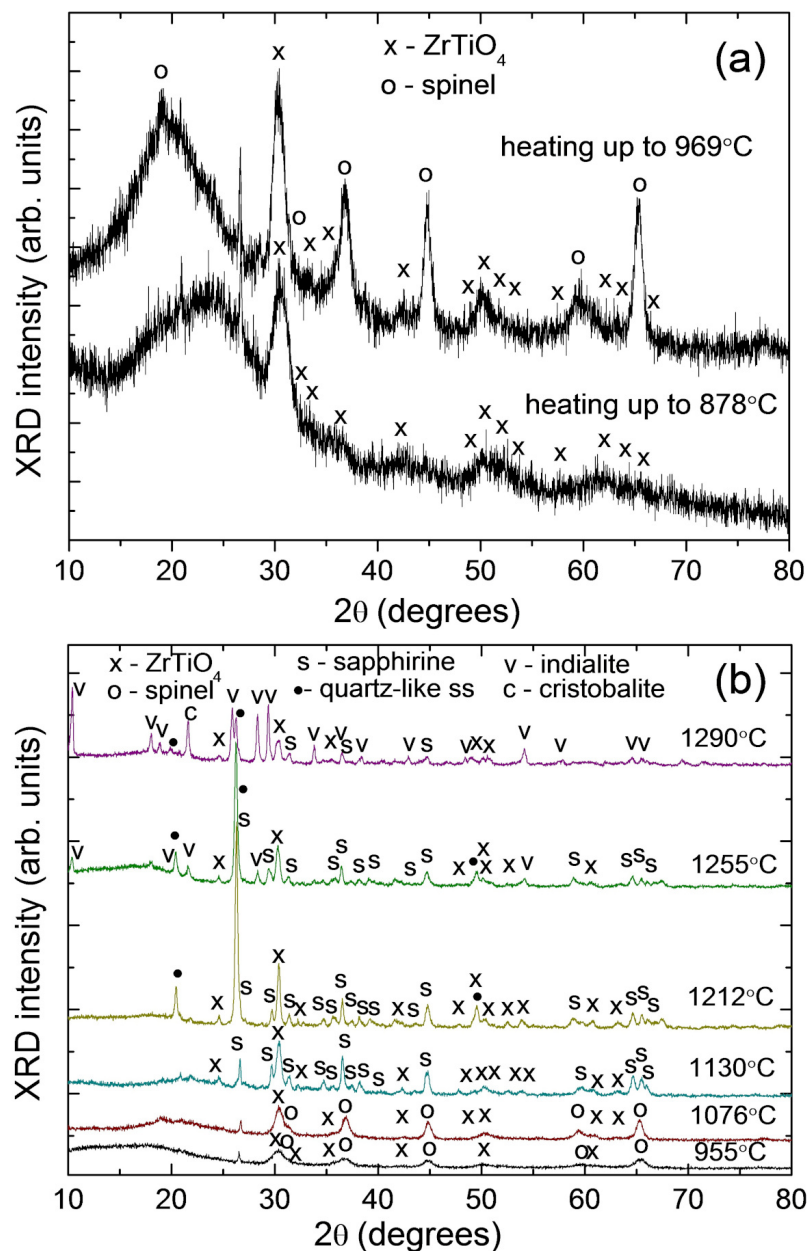
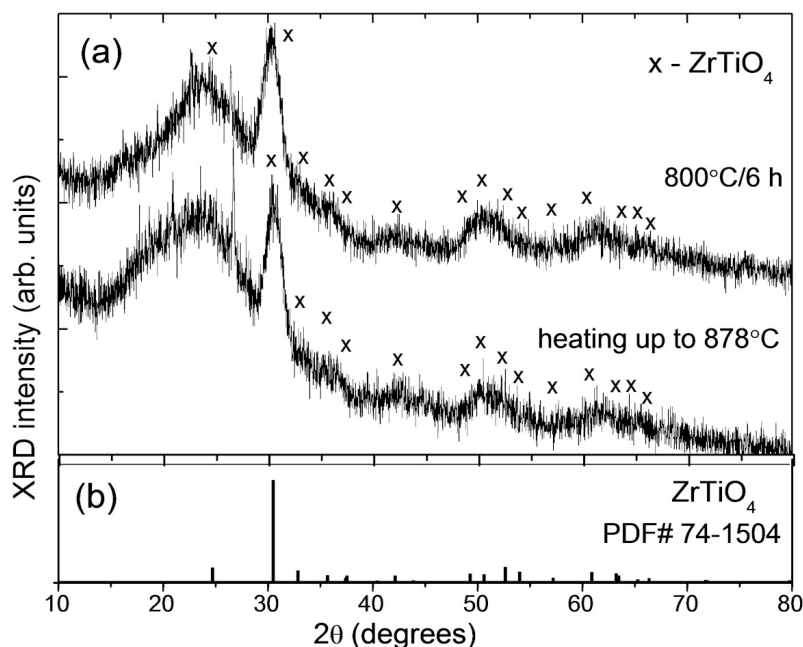


FIG. 3. XRD patterns (a) of the initial glass heat-treated in the DSC furnace up to 878 and 969 °C; (b) of the samples preheated at 800 °C for 6 h and heat-treated in the DSC furnace up to 955, 1076, 1130, 1212, 1255, and 1290 °C. The patterns are shifted for the convenience of observation

TABLE 1. The average crystal sizes D and spinel unit cell parameter a in glass-ceramics

Heat-treatment schedule	Spinel		ZrTiO ₄	Sapphirine	Indialite	Cristobalite
	D , nm	a , ± 0.003 , Å	D , nm	D , nm	D , nm	D , nm
800 °C/6 h	–	–	6.0	–	–	–
800 °C/6 h + 850 °C/6 h	8.5	8.068	6.0	–	–	–
800 °C/6 h + 900 °C/6 h	9.5	8.098	6.5		–	–
800 °C/6 h + 950 °C/6 h	12.0	8.099	8.0			
800 °C/6 h + 1000 °C/6 h	13.5	8.093	9.5	17.5	–	–
800 °C/6 h + 1050 °C/6 h	–	–	14.5	24.0	–	–
800 °C/6 h + 1100 °C/6 h	–	–	22.5	25.0	–	–
800 °C/6 h + 1200 °C/6 h	–	–	30.5		29.0	31.5
800 °C/6 h + 1300 °C/6 h	–	–	26.0		25.0	34.5

FIG. 4. (a) XRD patterns of the quenched glass heated in the DSC furnace up to 878 °C and the glass heat-treated at 800 °C for 6 h; (b) the standard pattern of ZrTiO₄

In the high temperature range of heat-treatments, at 1200 and 1300 °C, the residual glass crystallizes with the formation of crystals of stable phases of indialite, $2\text{MgO}\cdot 2\text{Al}_2\text{O}_3\cdot 5\text{SiO}_2$, and cristobalite, SiO_2 , while preserving sapphirine and zirconium titanate, see Fig. 5(a). Crystals of magnesium aluminosilicates with the quartz-like structure, which is observed in the DSC run, are not observed in glass-ceramics prepared in isothermal conditions. It is probably related to the selected heat-treatment schedules. We speculate that this phase will crystallize during heat-treatments in the temperature range from 1100 to 1200 °C.

Figure 5(b) shows the details of the formation of crystalline phases in transparent glass-ceramics. The position of the maximum of amorphous halo is located at $2\theta = 24.3^\circ$ in the XRD pattern of the initial glass. With increasing the heat-treatment temperature, it constantly shifts to $2\theta = 21.8^\circ$, the position of the maximum of amorphous halo in quartz glass, see Fig. 5(b). The characteristics of the crystalline phases formed during the heat-treatments are presented in Table 1.

Figure 6 demonstrates the Raman spectra of the initial glass and transparent glass-ceramics. The spectrum of the initial glass is typical for aluminosilicate glasses nucleated by a mixture of TiO_2 and ZrO_2 [9] and contains three broad Raman bands at ~ 450 , 800 and $\sim 920 \text{ cm}^{-1}$. The band at $\sim 920 \text{ cm}^{-1}$ is related to $[\text{TiO}_4]$ tetrahedra in the aluminosilicate network, while the bands with lower frequencies are the characteristics of the vibrations of the aluminosilicate network itself. After the heat-treatment of the initial glass at 800 °C for 6 h, intensity of the $\sim 920 \text{ cm}^{-1}$ band in its Raman

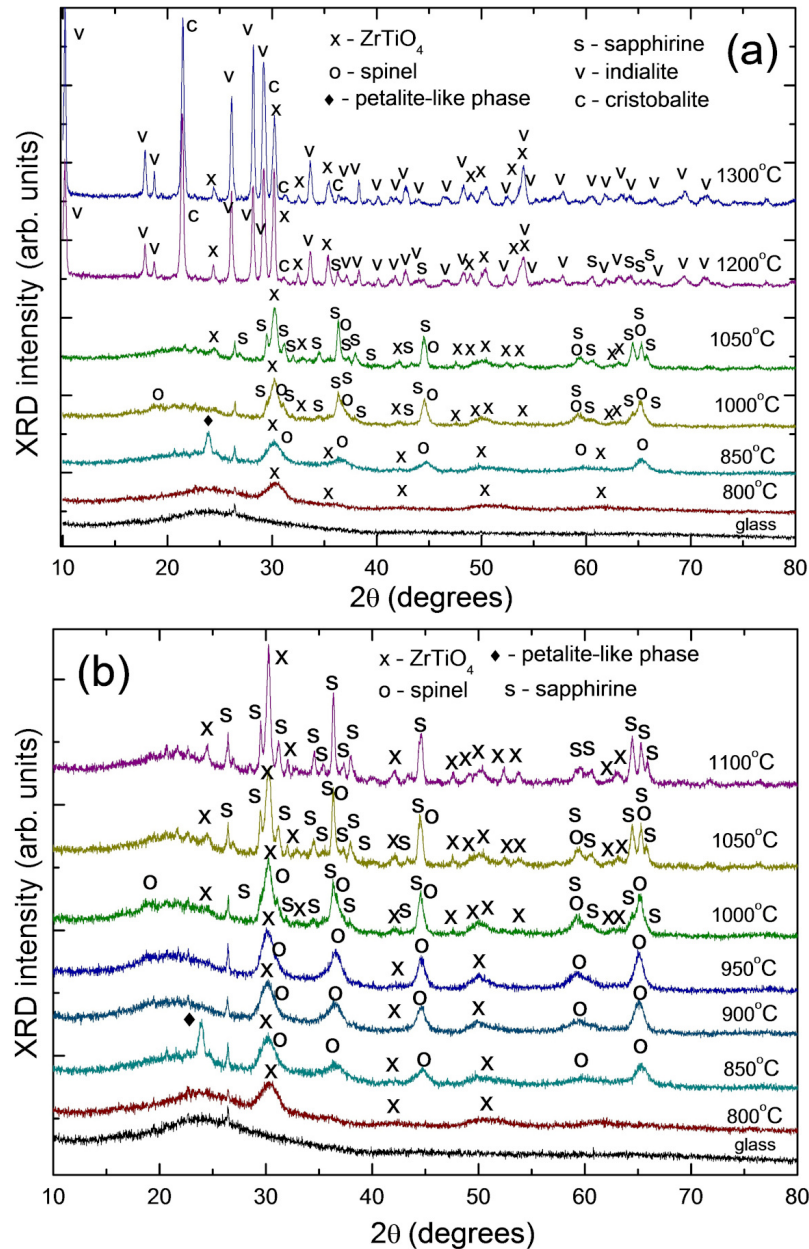


FIG. 5. (a,b) XRD patterns of the initial glass and glass-ceramics. (a) The heat-treatment temperature is from 800 to 1300 °C; (b) The heat-treatment temperature is from 800 to 1000 °C. Labels 850–1300 °C indicate the heat-treatment temperature at the second stage. Holding time at the second stage is 6 h. The nucleation stage is at 800 °C for 6 h

spectrum diminishes while intensity of the $\sim 800\text{ cm}^{-1}$ band goes up; the spectral features of $ZrTiO_4$ crystals [10–12] are clearly seen in the spectra (the characteristic bands locate at $\sim 154, 269, 334, 416$ and 645 cm^{-1}). The redistribution of intensities of the bands located in the high-frequency region in favor of the band centered at $\sim 790\text{ cm}^{-1}$ is the evidence of the development of phase separation [12]. In Raman spectra of glass-ceramics, the heat-treatment temperature increasing causes a further rise of the band at $\sim 800\text{ cm}^{-1}$ and bands related to the continuous precipitation of $ZrTiO_4$. The Raman bands typical for spinel nanocrystals with a partly inverse structure appear at $414, 488, 657, 724,$ and 796 cm^{-1} [10, 11]. In the spectrum of glass-ceramics prepared by the two-stage heat-treatment with the second stage at 1000 and 1050 °C, the Raman bands of sapphire appear at $457, 564,$ and 684 cm^{-1} [13]. Appearance of weak high-frequency bands at 940 and 1100 cm^{-1} in spectra of all glass-ceramics prepared by high-temperature heat-treatments is related to the vibrations of $[TiO_4]$ groupings in the residual highly siliceous glass [14].

Absorption spectra of the initial and heat-treated glasses are formed by an absorption edge located in the UV region of the spectrum, a broad intense unstructured band in the visible spectral range, a broad weak unstructured band with a maximum at $\sim 1000\text{ nm}$, a strong band with a maximum at $\sim 2000\text{ nm}$, and an absorption band in the region from 2700 to 3300 nm, see Fig. 7(a). In the spectrum of the glass, the position of the absorption edge corresponds to $\lambda = 362\text{ nm}$. A

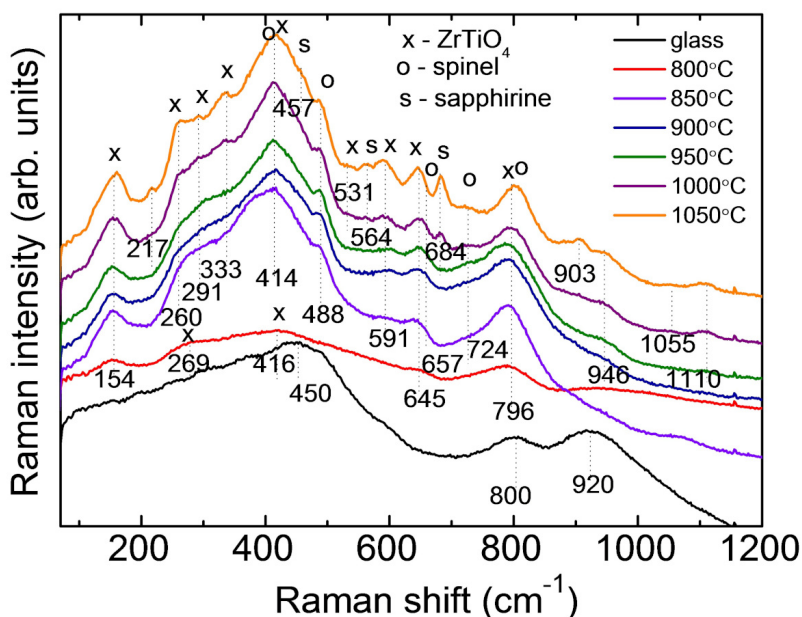


FIG. 6. Raman spectra of the initial glass and transparent glass-ceramics. Labels 850–1050 °C indicate the heat-treatment temperature at the second stage. The first stage is at 800 °C. The holding time at each stage is 6 ° h. $\lambda_{exc} = 514$ nm. Numbers denote the position of the Raman peaks in cm^{-1} . The curves are shifted for the convenience of observation

broad band with a maximum at ~ 1100 nm has absorption coefficient of $\sim 5.2 \text{ cm}^{-1}$. This absorption is mainly due to the ${}^5T_2 \rightarrow {}^5E({}^5D)$ transition of ferrous ions, Fe^{2+} , in octahedral ligand field (LF). The spectrum of the sample obtained by the heat-treatment at 800 °C for 6 h is similar to that of the initial glass, which means that crystallization of ZrTiO_4 does not involve iron ions. The absorption spectrum changes with spinel crystallization in the temperature region from 850 to 1000 °C. The absorption in the visible spectral range is caused by the oxygen to metal charge transfer (OMCT) $\text{O}^{2-}-\text{Fe}^{2+}$, $\text{O}^{2-}-\text{Fe}^{3+}$, $\text{O}^{2-}-\text{Ti}^{3+}$, $\text{O}^{2-}-\text{Ti}^{4+}$, as well as intervalent charge transfer (IVCT) $\text{Fe}^{2+}/\text{Fe}^{3+}$ and $\text{Ti}^{4+}-\text{Fe}^{2+}$ bands. We cannot rule out a weak absorption of Fe^{3+} and Ti^{3+} ions in octahedral ligand field. A broad band at 1500–2200 nm with a maximum at $\sim 1.90 \mu\text{m}$ appears and grows with increasing the heat-treatment temperature while the band with a maximum at ~ 1100 nm decreases in intensity. An appearance and growth of the band at 1500–2200 nm is due to the entry of Fe^{2+} ions into spinel nanocrystals in the tetrahedral positions (T_d) (the ${}^5E \rightarrow {}^5T_2({}^5D)$ transition).

With the increase of the heat-treatment temperature up to 1050 °C, in the spectrum of glass-ceramics a noticeable drop in the intensity of the absorption band in the region of 2000 nm associated with Fe^{2+} ions in T_d sites in spinel is observed. This correlates with the decrease in the amount of spinel nanocrystals and appearance of sapphire. In sapphire, Mg^{2+} ions are in sixfold coordination while Al^{3+} ions are in four- and sixfold coordinated sites [15]. Sapphire is known to accommodate iron ions. There are the substitutions $\text{Mg}^{2+} \rightarrow \text{Fe}^{2+}$ (predominantly) and $\text{Al}^{3+} \rightarrow \text{Fe}^{3+}$ with Fe^{3+} ions assigned to tetrahedral positions [16]. Thus, upon sapphire formation from spinel and residual highly siliceous glass, iron ions are present as the ${}^{IV}\text{Fe}^{3+}$ and ${}^{VI}\text{Fe}^{2+}$ species [4]. It is reflected in the absorption spectrum of glass-ceramic obtained by the heat-treatment at 1050 °C, see Fig. 7. The structuring of the spectrum of OH-groups is due to their incorporation into spinel nanocrystals [17].

4. Conclusions

Model glass of the $\text{MgO} - \text{Al}_2\text{O}_3 - \text{SiO}_2$ ternary system intended for the development of transparent glass-ceramics based on the $\text{Fe}^{2+}:\text{MgAl}_2\text{O}_4$ spinel nanocrystals was nucleated by a mixture of TiO_2 and ZrO_2 and doped with 0.6 mol% FeO . The glass was melted at 1580 °C for 4 h with stirring and heat-treated in the temperature range from 800 to 1300 °C.

The structure, phase composition and spectroscopic properties of the initial glass and glass-ceramics were studied by the differential scanning calorimetry and X-ray diffraction analysis, Raman and absorption spectroscopy.

ZrTiO_4 nanocrystals 6 nm in size precipitate in the glass during its nucleation heat-treatment at 800 °C. Similar crystal fraction of ZrTiO_4 appears during heating of the initial glass to the temperature of ~ 880 °C. Spinel nanocrystals appear during two different heat-treatment protocols, i.e., in the course of heating of the initial glass up to the temperature of 970 °C and by the two-stage heat-treatments with temperature from 850 to 1000 °C at the second stage. Spinel nanocrystals with average size ranging from 9 to 14 nm and with unit cell parameter $a = 8.068 - 8.099 \text{ \AA}$ are formed in glass-ceramics during heat-treatments at temperatures from 850 to 1000 °C. A broad absorption band spanning from ~ 1.5 to $2.5 \mu\text{m}$ is assigned to the ${}^5E \rightarrow {}^5T_2({}^5D)$ transition of Fe^{2+} ions in T_d sites in spinel nanocrystals.

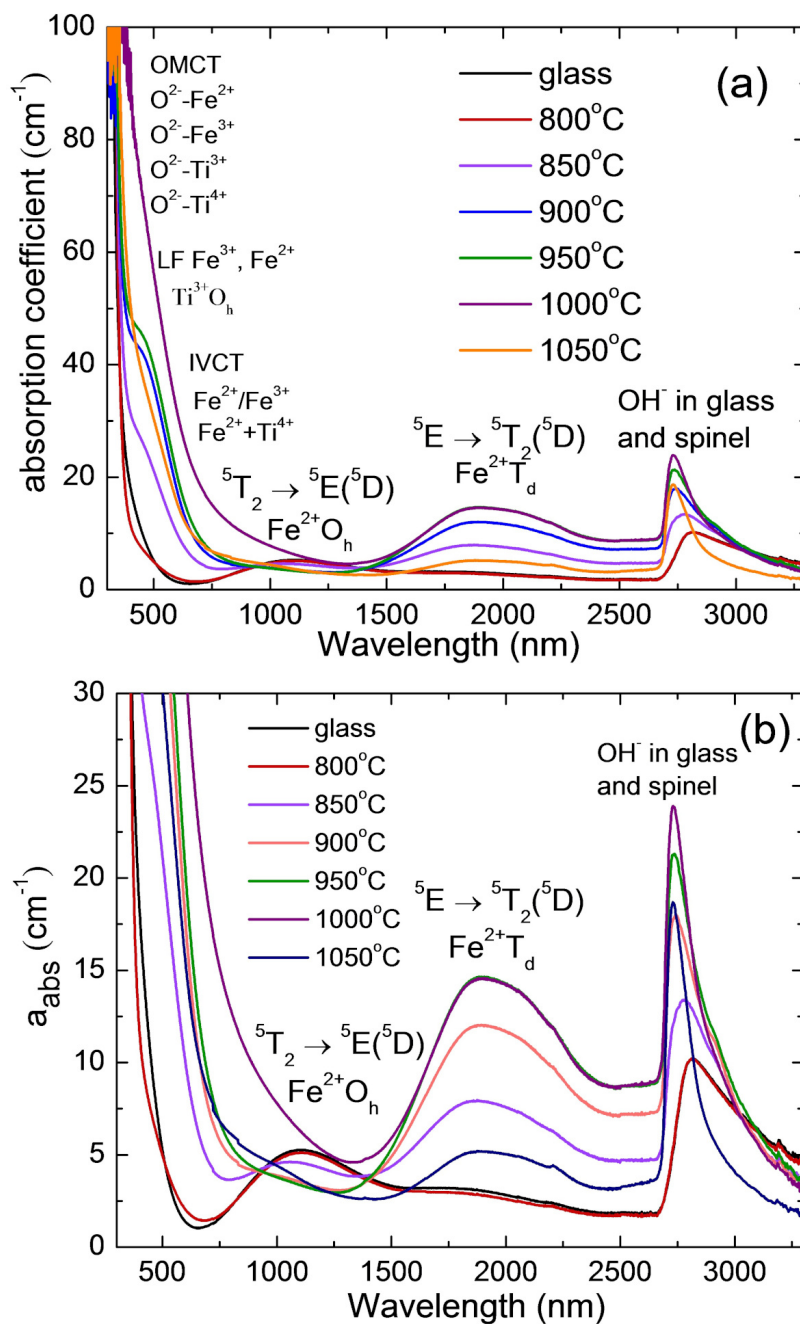


FIG. 7. Absorption spectra of the glass and transparent glass-ceramics in different scales along the Y-axis. Labels 850–1050 °C indicate the heat-treatment temperature at the second stage. The first stage of the heat-treatment is always at 800 °C for 6 h

Iron-doped sapphirine nanocrystals with average sizes ranging from 18 to 25 nm appear in glass-ceramics during heat-treatments from 1000 to 1100 °C. Appearance of iron-doped sapphirine nanocrystals results in a decrease of absorption in the spectral range from ~ 1.5 to $2.5 \mu\text{m}$. The obtained regularities are important for the development of saturable absorbers for the spectral range of $2\text{--}3 \mu\text{m}$.

References

- [1] Frolov M.P., Korostelin Yu.V., Kozlovsky V.I., Podmar'kov Yu.P., Savinova S.A., Skasyrsky Ya.K. 3 J. pulsed Fe:ZnS laser tunable from 3.44 to 4.19 μm . *Laser Phys. Lett.*, 2015, **12**(5), P. 055001(1-6).
- [2] Basyrova L., Balabanov C., Belyaev A., Drobotenko V., Vitkin V., Dymshits O., Loiko P. Synthesis, structure and spectroscopy of Fe^{2+} : MgAl_2O_4 transparent ceramics. *J. Phys.: Conf. Ser.*, 2019, **1410**, P. 012123(1-4).
- [3] Dymshits O., Shepilov, M., Zhilin A. Transparent glass-ceramics for optical applications. *MRS Bulletin*, 2017, **42**, P. 200–205.
- [4] Basyrova L., Bukina V., Balabanov S., Belyaev A., Drobotenko V., Dymshits O., Alekseeva I., Tsenter M., Zapalova S., Khubetsov A., Zhilin A., Volokitina A., Vitkin V., Mateos X., Serres J.M., Camy P., Loiko P. Synthesis, structure and spectroscopy of Fe^{2+} : MgAl_2O_4 transparent ceramics and glass-ceramics. *J. Lumin.*, 2021, **236**, P. 118090(1-17).

- [5] Dugué A., Dymshits O., Cormier L., Cochain B., Lelong G., Zhilin A., Belin S. In situ evolution of Ni environment in magnesium aluminosilicate glasses and glass–ceramics. Influence of ZrO₂ and TiO₂ nucleating agents. *J. Phys. Chem. Solids*, 2015, **78**, P. 137–146.
- [6] Golubkov V.V., Dymshits O.S., Zhilin A.A., Chuvaeva T.I., Shashkin A.V., On the phase separation and crystallization of glasses in the MgO–Al₂O₃–SiO₂–TiO₂ system. *Glass Phys. Chem.*, 2003, **29**, P. 254–266.
- [7] Carl G., Höche T., Voigt B. Crystallisation behavior of a MgO–Al₂O₃–SiO₂–TiO₂–ZrO₂ glass. *Phys. Chem. Glasses.*, 2002, **43C**, P. 256–258.
- [8] Lipson H., Steeple H., in: McMillan (Ed.), *Interpretation of X-Ray Powder Patterns*, Martins Press, London, N.Y., 1970, p. 344.
- [9] Loiko P.A., Dymshits O.S., Zhilin A.A., Alekseeva I.P., Yumashev K.V. Influence of NiO on phase transformations and optical properties of ZnO–Al₂O₃–SiO₂ glass–ceramics nucleated by TiO₂ and ZrO₂. Part II. Optical absorption and luminescence. *J. Non-Cryst. Solids*, 2013, **376**, P. 99–105.
- [10] Krebs M.A., Condrate R.A. A Raman spectral characterization of various crystalline mixtures in the ZrO₂–TiO₂ and HfO₂–TiO₂ systems, *J. Mater. Sci. Lett.*, 1988, **7**, P. 1327–1330.
- [11] Azough F., Freer R., Petzelt J. A Raman spectral characterization of ceramics in the system ZrO₂–TiO₂. *J. Mater. Sci.*, 1993, **28**, P. 2273–2276.
- [12] Alekseeva I.P., Dymshits O.S., Golubkov V.V., Loiko P.A., Tsenter M.Ya., Yumashev K.V., Zapalova S.S., Zhilin A.A. Influence of NiO on phase transformations and optical properties of ZnO–Al₂O₃–SiO₂ glass–ceramics nucleated by TiO₂ and ZrO₂. Part I. Influence of NiO on phase transformations of ZnO–Al₂O₃–SiO₂ glass–ceramics nucleated by TiO₂ and ZrO₂. *J. Non-Cryst. Solids*, 2014, **384**, P. 73–82.
- [13] Lamara S., Redaoui D., Sahnoune F., Heraiz M., Saheb N., Microstructure, thermal expansion, hardness and thermodynamic parameters of cordierite materials synthesized from Algerian natural clay minerals and magnesia. *Bol. Soc. Esp. Cerám. V.*, 2021, **60**(5), P. 291–306.
- [14] Alekseeva I., Dymshits O., Ermakov V., Golubkov V., Malyarevich A., Tsenter M., Zhilin A., Yumashev K. *Phys. Chem. Glasses Eur. J. Glass Sci. Technol. B*, 2012, **53**(4), P. 167–180.
- [15] Povarennykh A.S. *Crystal Chemical Classification of Minerals*. Springer, New York, 1972, p. 286.
- [16] Steffen G., Seifert F., Amthauer G. Ferric iron in sapphirine: a Mössbauer spectroscopic study. *Am. Mineral.*, 1984, **69**, P. 339–348.
- [17] Bromiley G.D., Nestola F., Redfern S.A.T., Zhang M., Water incorporation in synthetic and natural MgAl₂O₄ spinel. *Geochem. Cosmochim. Acta*, 2010, **74**, P. 705–718.

Submitted 10 October 2023; accepted 14 November 2023

Information about the authors:

Vasilisa S. Bukina – Vavilov State Optical Institute, 36 Babushkina St., St. Petersburg, 192171, Russia; ORCID 0009-0006-3752-0722; nakara.oriara@mail.ru

Olga S. Dymshits – Vavilov State Optical Institute, 36 Babushkina St., St. Petersburg, 192171, Russia; Ioffe Institute, 26 Politekhnicheskaya, St Petersburg, 194021, Russia; ORCID 0000-0003-1980-0561; vodym1959@gmail.com

Irina P. Alekseeva – Vavilov State Optical Institute, 36 Babushkina St., St. Petersburg, 192171, Russia; vgolub19@gmail.com

Anna A. Volokitina – Vavilov State Optical Institute, 36 Babushkina St., St. Petersburg, 192171, Russia; ORCID 0000-0002-6091-6534; anna.itmo@gmail.com

Svetlana S. Zapalova – Vavilov State Optical Institute, 36 Babushkina St., St. Petersburg, 192171, Russia; zenii99@yandex.ru

Aleksandr A. Zhilin – D.V. Efremov Institute of Electrophysical Apparatus, 3 Doroga na Metallostroi, pos. Metallostroi, St Petersburg, 196641, Russia; zhilin1311@yandex.ru

Conflict of interest: the authors declare no conflict of interest.